ACS APPLIED BIO MATERIALS

www.acsabm.org Article

Silk Fibroin Microneedle Patches for the Sustained Release of Levonorgestrel

Burcin Yavuz,[§] Laura Chambre,[§] Kristin Harrington, Jonathan Kluge, Livio Valenti, and David L. Kaplan*

Cite This: *ACS Appl. Bio Mater.* 2020, 3, 5375−5382 Read Online

ACCESS | Metrics & More | Article Recommendations

ABSTRACT: The sustained release of levonorgestrel, a contraceptive, from silk-based microneedle patches was demonstrated for transdermal delivery. Modifications in the formulation of the silk protein and drug loading enabled the tuning of drug loading and release rates from the microneedle patches over time. Sustained drug release reached up to 100 days when the drug was loaded directly inside the microneedles, while release continued for more than a year when the drug was loaded inside microparticles prior to casting inside the microneedle patches. When coupled with the shelf-stable, refrigeration-less features of the silk protein matrix utilized in the microneedle fabrication, these findings suggest that long-acting contraception patches are feasible. This advance could provide practical options for women to have access to new options for protection against unwanted pregnancy.

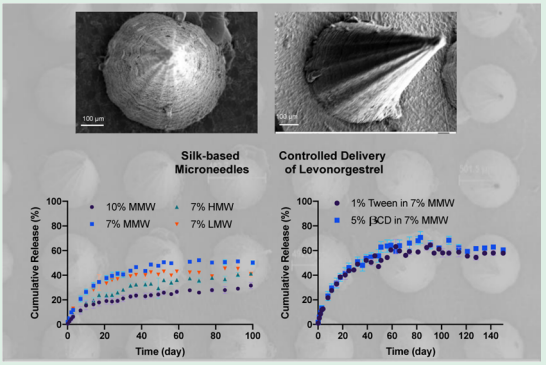

KEYWORDS: *silk fibroin, microneedles, contraception, levonorgestrel, sustained release*

INTRODUCTION

Voluntary family planning has contributed to advances in public health and to a woman's options regarding reproduction. Women can make the decision about having children, contributing to the diminution of unwanted pregnancies and newborn deaths.[1] However, due to the limited choice of methods and access to contraception, as well as cultural or religious constraints, approximately 214 million women in developing countries have limited access to contraceptives and family planning.[1] For example, the use of modern contraceptives is accessible to less than 20% of women in Sub-Saharan Africa and one-third of women in Southeast Asia. Globally, between 2010 and 2014, 44% of pregnancies were unwanted; of which 25% resulted in unsafe abortions.[2,3] To ensure the safety and well-being of all women, access to family planning and modern contraceptive methods is critical.

Transdermal microneedle (MN) patches are a painless method of drug delivery, offering a preferred administration route over injection. MN patches penetrate the skin barrier and deliver therapeutics like proteins, peptides, vaccines, and small molecules.[4] Compared to oral delivery, where more extreme chemical conditions in the gastrointestinal tract can result in the degradation of protein-based drugs, transdermal delivery avoids these problems, enabling absorption via dermal circulation.[5−7] MNs are noninvasive and pain-free modes of drug administration, thus increasing patient acceptance and compliance. However, biocompatible materials and control over the release profile of drugs remain a challenge, particularly with respect to long-term sustained release and safety.[8,9] New delivery systems to overcome these limitations would enhance the therapeutic portfolio of transdermal drug delivery options. Recently, an MN patch based on poly(lactic acid) (PLA) and poly(lactide-coglycolide acid) (PLGA) was developed for the sustained release of the contraceptive hormone levonorgestrel (LVN).[10] The majority of the drug delivery systems on the market currently use synthetic polymers such as the PLA and PLGA, yet natural polymers such as collagen and silk proteins generate useful alternatives, including noninflammatory degradation products and aqueous processing conditions to enhance the retention of bioactive features of the drugs to be delivered.[11,12]

Silk protein is a structural protein utilized in FDA-approved medical devices, safe in humans, fully degradable over time, and can be formed into mechanically robust materials. This protein provides a versatile set of options in terms of material formats and structures that can be manipulated with respect to drug stability and delivery due to the high molecular amphiphilic nature of the silk protein polymer, including the release kinetics.[13] Tunable drug release and nontoxic degradation

Received: June 3, 2020
Accepted: July 7, 2020
Published: July 7, 2020

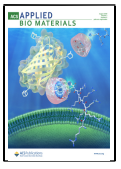

https://dx.doi.org/10.1021/acsabm.0c00671
ACS Appl. Bio Mater. 2020, 3, 5375−5382

products (amino acids) have prompted the study of silk fibroin from silkworms for drug delivery systems.[14−16] Multiple release studies with antibiotics, chemotherapeutic drugs, and antibodies demonstrated the ability of silk to sequester, stabilize, and to provide sustained release of therapeutic molecules ranging from small molecule to complex proteins using a diverse set of silk material delivery formats such as foam, films, gels, tubes, and particles.[17−22] Previously, we demonstrated the fabrication of high-aspect-ratio silk MNs and showed the release of large molecules and antibiotics with these systems.[23] Silk-based MNs arrays were used for the successful delivery of vaccines against human immunodeficiency virus (HIV), influenza, *Clostridium difficile*, and *Shigella*.[24−26] The main advantages of silk-based MN patch delivery systems include drug stabilization in the matrices to provide shelf-stable material systems without a need for refrigeration, processing of the silk and drug into MN patches in aqueous media to support the retention of drug bioactivity, degradation of the patches in vivo without inflammatory degradation products, preservation of the bioactivity of peptides and complex proteins formulated in the silk, formation of depot release reservoirs in the dermal space to sustain delivery, and modulation of the release kinetics of the drug by changing silk processing methods.

In the present study, we report the fabrication of silk-based MN patches for the sustained delivery of LVN, a synthetic progestin used in contraception and hormone therapy. We demonstrate that different loadings of the drug, such as via pre-encapsulation in silk microparticles (MPs) or freely inside the MNs, the release kinetics of the drug can be tuned. Moreover, to provide further control of the release profiles, different molecular weights of the silk, as well as the use of solubility enhancers, were utilized in the study to further modulate release kinetics and sustained release of the drug.

MATERIALS AND METHODS

Silk Fibroin Isolation. Silk fibroin was isolated from *Bombyx mori* cocoons as previously described.[27] Briefly, silk fibroin protein was extracted from *Bombyx mori* cocoons (Tajima Shoji Co., Japan) by boiling in a 0.02 M sodium carbonate solution for 30, 60, or 120 min (hereafter referred to as low molecular weight (LMW), medium molecular weight (MMW), and high molecular weight (HMW), respectively) to remove the sericin.[28] The extracted silk fibroin was then dried for 12 h in a chemical hood before being dissolved in a 9.3 M LiBr solution at 60 °C for 4 h for solubilization, yielding a 20% w/v solution. This solution was dialyzed against distilled water using Pierce Slide-a-Lyzer cassettes, MWCO 3500 Da (Rockford, IL) for 3d to remove the LiBr. The solution was centrifuged (14 000 rpm, 20 min cycle) to remove aggregates formed during purification. The final concentration of the aqueous silk fibroin (hereafter referred to as SF) was ∼6−8% w/v.

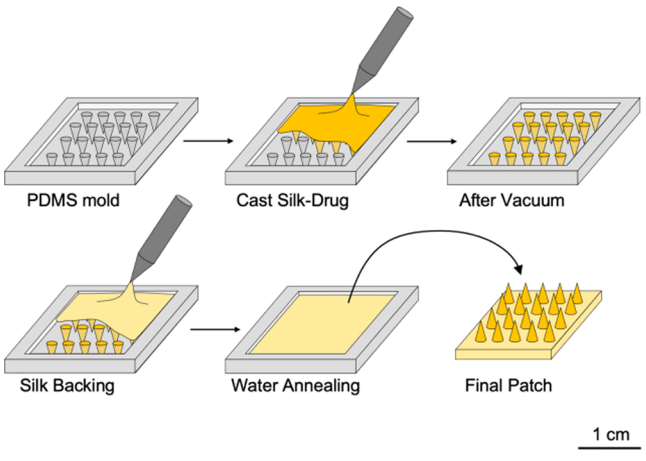

Figure 1. Fabrication process for LVN-loaded silk fibroin MNs. PDMS molds were filled with the silk-LVN solution and placed under vacuum to force material into the needle voids. Additional silk was subsequently added for the robust backing after overnight drying under ambient conditions. Silk MNs were water annealed and demolded to obtain a patch of 1.5 × 1.5 cm^2, comprised of 400 needles, each with a length of 700 μm and a base of 400 μm.

Preparation of Silk Fibroin Microparticles. To prepare silk MPs, the silk solution was diluted in water to 6 wt %, and 3 mL of this solution was mixed with 12 mL of 5 wt % poly(vinyl alcohol) (PVA, Sigma, St. Louis, MO) solution. After mixing, the solution was transferred to open polystyrene petri dishes (100 mm), and all dishes were placed in a fume hood to dry overnight.[29] The dried films were then peeled off the dish and the poly(vinyl alcohol) was dissolved in phosphate-buffered saline (PBS), and the solution was centrifuged to obtain the residual silk MPs. The MP pellet washed with PBS and resuspended for lyophilization. Levonorgestrel (LVN, Sigma, St. Louis, MO) was suspended in ethanol (EtOH, Sigma, St. Louis, MO) and incubated with microparticles at 10% (wt/wt) of total MP amount for 3 days using constant stirring. After 3 days, the caps of the vials were opened to allow the EtOH to evaporate. The drug-loaded MPs were then washed with EtOH to remove excess drug that were not bounded to the MPs and resuspended in PBS for lyophilizing.

Characterization of Silk Fibroin Microparticles. *Fourier Transform Infrared (FTIR) Spectroscopy.* Silk materials were analyzed for structural features via a JASCO FT-IR 6200 spectrometer (JASCO, Tokyo, Japan) combined with a MIRacle attenuated total reflection (ATR) germanium crystal. Background measurements were recorded before sample reading and subtracted from the sample spectrum. For each measurement, spectral scans were run from 1550 to 1750 cm^{-1} at a resolution of 2 cm^{-1} for 128 scans per sample. Three samples were measured for each group. The secondary structure was evaluated as we have previously reported.[30] Briefly, Fourier self-deconvolution (FSD) of the FT-IR spectra covering the amide I region (1590−1710 cm^{-1}) was performed using Opus 5.0 software. Spectra were deconvoluted using a Lorentzian line shape, a half- bandwidth between 25 and 26 cm^{-1}, a noise reduction factor of 0.3, and apodization with a Blackman−Harris function. A baseline correction for the deconvoluted amide I region was subtracted before curve fitting. For curve fitting, Gaussian line shape profiles were input at positions (in cm^{-1}) that correlated with the second derivative of the original spectra, and the input for peak width was kept constant at the software's default value of 6 cm^{-1} for all peaks. Eleven fitted bands were chosen to define the secondary structure of amide I. Assignments for each band were based on those in our prior report.[30] Relative areas of the single bands were used to determine the fraction of the structural element (N = 3, where three sets of scans were obtained for the same sample).

Particle Size Analysis. The particle size of the MPs was measured using a Microbrook 2000L (Brookhaven Instruments, Holtsville, NY) that combines laser diffraction and high-angle detection techniques and is capable of measuring a broad size range between 20 nm and 2000 μm. The sample was prepared according to the manufacturer's instructions. Reading was done following the manufacturer's instructions. Measurements were made using the Mie distribution method, and the results are presented as the cumulative size distribution of the MPs.[31]

Scanning Electron Microscopy (SEM) Analysis of Microparticles. SEM was performed to evaluate the morphology of the silk microparticles and LVN using a Zeiss EVO-10MA microscope (Zeiss, Oberkochen, Germany) at 5 kV accelerating voltage. Prior to imaging, the MP samples were fixed onto SEM sample holders using a carbon tape and then coated with ∼10 nm gold using a SC7620 sputter coater (Quorum Technologies, U.K.).

Preparation of Silk Fibroin Microneedle Patches. Drop cast MNs were prepared using poly(dimethylsiloxane) (PDMS) molds as previously described.[24] The molds were patterned with a 20 × 20 array of conical MNs, each MN with a 700 μm height, 15 μm tip diameter,

https://dx.doi.org/10.1021/acsabm.0c00671
ACS Appl. Bio Mater. 2020, 3, 5375−5382

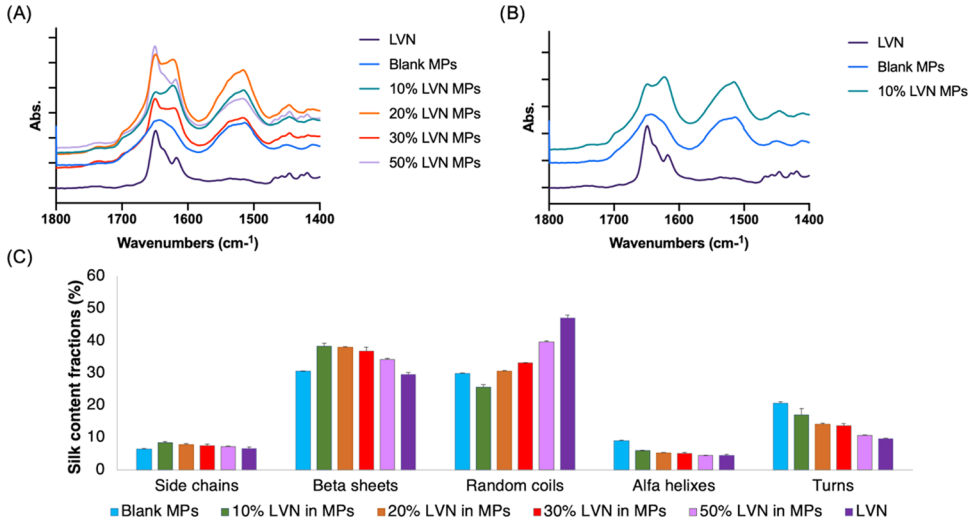

Figure 2. FTIR spectra: (A) MPs with different LVN ratios; (B) LVN, blank MPs, and LVN-loaded MPs; (C) percentage of the silk secondary structural content in formulations based on FTIR (all data represent mean ± SD for $n = 3$). LVN characteristic peak (2900 cm^{-1}) observed in LVN-loaded MPs spectrum (A), as an indication of the presence of nonencapsulated drug. LVN characteristic C═O peak overlaps with silk random coil peaks around 1650 cm^{-1} (A), thus the random coil ratio in silk was higher for higher percentages of LVN where there is more free drug available. (C) β sheet content >30% for all formulations.

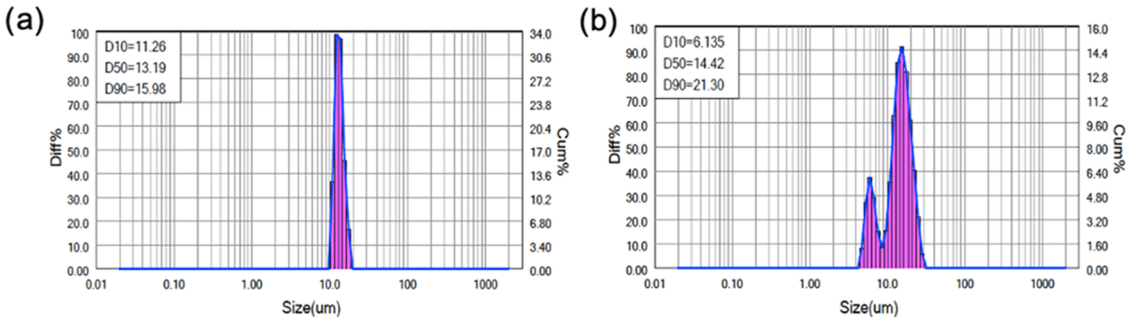

Figure 3. Particle size distributions of (a) HMW, 6% MPs and (b) MMW, 6% MPs. Results are presented as the cumulative size distribution of the MPs. D10 refers to the portion of particles with diameters smaller than this value, here 10%, D50 for 50%, and D90 90%. HMW MPs have a D50 (median diameter) value of 13.19 μm with a span ((D90−D10)/D50) of 0.358, whereas medium MW MPs have a D50 value of 14.42 μm with a span of 1.052.

and 360 μm base diameter. In total, 5 mg/mL of powder LVN or an equivalent amount of silk MPs were mixed with MMW 7% silk. Alternatively, to prepare high-dose LVN-MNs, 20 mg/mL of LVN was mixed with 7% MMW silk with 3% dimethyl sulfoxide (DMSO). The dose of LVN was chosen for 6 months sustained release with a daily dose of 25−30 μg per day.[32] In addition, different molecular weights of silk were tested in terms of drug release properties (LMW, MMW, and HMW) as well as different silk concentrations (7 and 10%). Finally, solubility enhancer such as β-cyclodextrin (5% w/v) and a surfactant (Tween-20, 1% v/v) were added to the MMW silk-drug solution prior to casting to study their effect on the release profile of the LVN from the patches. For example, for an MN made of MMW 7% silk containing 20 mg of LVN and 3% DMSO, we prepared a 5 mL of stock solution containing 100 mg of LVN, 150 μL of DMSO, and 4.85 mL of silk solution (7%, MMW). When Tween or β-cyclodextrin was used, 50 μL or 250 μg, respectively, was added to that stock solution. Then, 500 μL of this stock solution was cast into the PDMS molds (Figure 1). The molds were placed into a vacuum oven, and vacuum was applied for 5 min at room temperature to remove any bubbles. The vacuum was released for 20 s and then reapplied. This vacuum cycling process was repeated 4−5 times until there were no remaining bubbles and all of the indents were filled with the silk mixture. The MN patches were dried overnight on the bench-top and then removed from the molds using tweezers, followed by water vapor annealing to increase the crystallinity of the MNs.[33]

Differential Scanning Calorimetry (DSC) Analysis. DSC analysis was used to confirm LVN entrapment in the silk MNs. Approximately, 10 mg of LVN or MN samples were hermetically sealed in aluminum pans (TA Instruments, New Castle, DE) and loaded into a Q100 DSC (TA Instruments) with a dry nitrogen gas flow of 50 mL/min at a speed rate of 10°/min.

In Vitro Release Studies. The in vitro release kinetics of LVN from the silk MPs was tested under sink conditions, where the release media used was able to dissolve at least 3 times the amount of LVN that is in the samples. To maintain sink conditions throughout the release studies, 5 mg of MPs containing a total of 0.5 mg of LVN were placed in a Slide-A-Lyzer MINI Dialysis Device (3500 kDa) in 45 mL of 0.5% sodium dodecyl sulfate (SDS) solution, where a dialysis membrane separated the MPs from the release medium to prevent MP loss during sampling. The tubes were incubated at 37 °C without shaking. The in vitro LVN release studies from the silk MN patches were also performed using 1 mL of PBS (nonsink conditions) at 37 °C without any shaking. For the nonsink conditions, all media was collected at specific sampling time points and replaced with fresh medium, while for the sink conditions, 1 mL of sample was collected and replaced with a fresh medium. Moreover, in the case of sink conditions, patches were immersed in 200 mL of PBS or 5% SDS as indicated, and at each time point, 1 mL of the media was recovered for analysis and replaced with 1 mL of fresh buffer. Sink conditions are more appropriate for release studies for drugs with poor aqueous solubility, such as LVN, while

https://dx.doi.org/10.1021/acsabm.0c00671
ACS Appl. Bio Mater. 2020, 3, 5375−5382

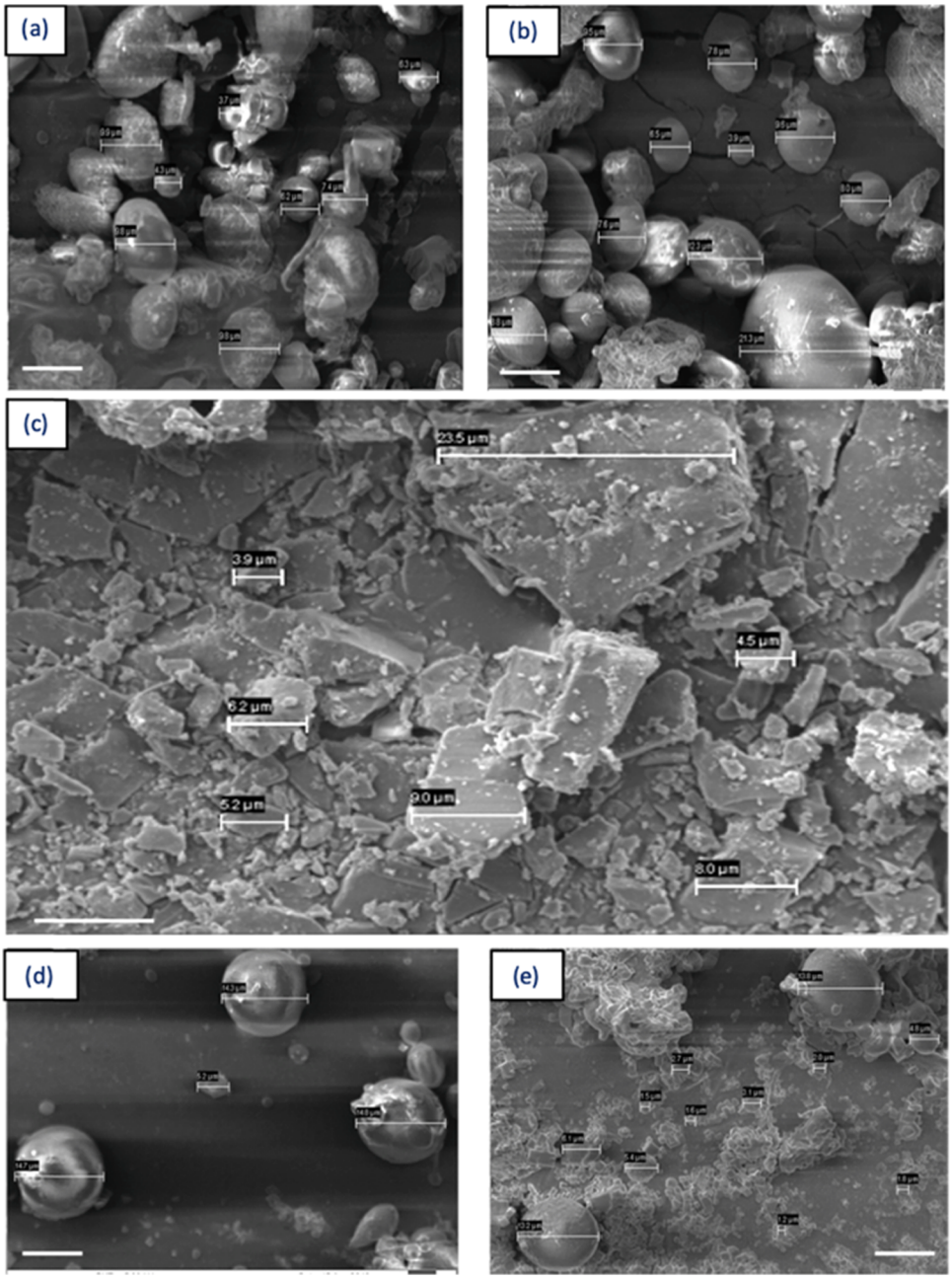

Figure 4. Figure rearranged, SEM micrographs showing structure and sizes of: (a) LVN-loaded HMW MPs, (b) LVN-loaded LMW MPs, (c) LVN alone, (d) blank HMW MPs, and (e) blank LMW MPs. Micron-size crystalline structure of LVN (c) can be detected in LVN-loaded MP micrographs (a, b) as well, indicating the presence of free drug attached on particle surfaces and not encapsulated. The particle size distribution of MPs prepared with the MMW silk was more homogeneous (d) when compared to the LMW MPs, as also seen in the particle size distribution data (Figure 3). Scale bars are 10 μm.

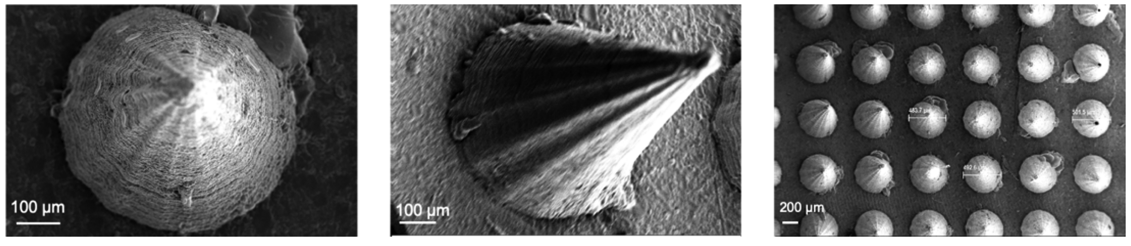

Figure 5. SEM micrographs showing the structure and size of LVN-loaded silk MNs (7%, HMW).

nonsink conditions were chosen for comparison.[10] The amount of LVN in the samples was quantified by liquid chromatography using a 1200 series high-performance liquid chromatography (HPLC, Agilent Technologies, Santa Clara, CA). An Agilent ZORBAX Eclipse Plus-

https://dx.doi.org/10.1021/acsabm.0c00671
ACS Appl. Bio Mater. 2020, 3, 5375−5382

C18 column (5 μm, 3 × 150 mm^2) (Agilent Technologies, Palo Alto, CA) was used with a column temperature at 25 °C. The mobile phase was optimized with acetonitrile:water with 0.1% trifluoroacetic acid (70:30) (Sigma, St. Louis, MO) with a 1 mL/min flow rate, and the UV detection was at 250 nm. To assess the quantity of LVN unreleased, the patches were immersed in DMSO and the media was analyzed via HPLC until no LVN was observed in HPLC chromatograms.

Stability Study. The stability of LVN inside the MNs was assessed under accelerated storage studies for 30 days at 40 ± 2 °C with 75 ± 5% relative humidity as recommended by FDA guidelines (Guidance for Industry Q1A(R2) for accelerated stability studies). Following incubation, MNs were incubated in DMSO and the extracted amount of LVN was quantified using HPLC.

RESULTS AND DISCUSSION

Fabrication and Characterization of Silk Fibroin Microparticles. Drug-loaded MPs were synthesized following the procedures we have previously described.[29] MP formation was obtained by exploiting the phase separation between poly(vinyl alcohol) (PVA) and silk that occurs spontaneously when the two polymers are mixed and cast into films. Subsequently, a solution of LVN in ethanol was incubated with the MPs for 3 days to ensure maximal loading and then allowed dry for the removal of ethanol. LVN is not soluble in water and has a solubility of 0.2 mg/mL in ethanol and 5 mg/mL in DMSO. To ensure total removal of the organic solvent, ethanol was used for the loading of the drug as the boiling point of DMSO is too high at 189 °C.

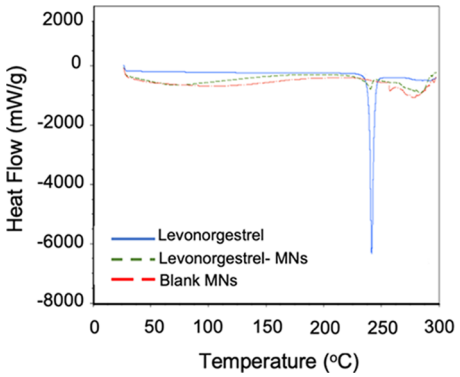

Figure 6. DSC thermograms for LVN alone (control), blank MNs (no drug, control), and LVN-loaded MNs (10 mg LVN).

Characterization of Silk Fibroin Microparticles. *Fourier Transform Infrared (FTIR) Spectroscopy.* The characteristic peaks of LVN are at 3300 (O−H stretching) and 1652 cm^{-1} (C═O stretching).[32] The C═O stretching occurs at the same wavelength as the region for silk random coils (1650 cm^{-1}) (Figure 2a,b). This interference renders FTIR analysis more complex as an increase in random coil (1638−1655 cm^{-1}) as well as β-sheet (1622−1637 cm^{-1}) content, compared to silk alone, was observed with increased LVN ratios in the MPs, indicating the presence of increased levels of unbound LVN (Figure 2c). Hence, the increase in random coil and β-sheet content correlated with the amount of LVN loaded inside the MPs.

Particle Size Analysis. Particle size measurements showed that the HMW silk MPs had more uniform particle size distributions, with an average of 13.2 μm with a span of 0.358. Particle sizes of the MMW silk MPs ranged of 6.1−21.3 μm with an average of 14.42 μm with a span of 1.052 (Figure 3).

Scanning Electron Microscopy (SEM) Analysis of Microparticles. SEM images of LVN showed micron-size structures of LVN (Figure 4c). The SEM micrographs supported the particle size measurements as the particle size distribution was narrower when HMW silk was used to prepare the MPs (Figure 4d,e). According to Figure 4b, free LVN particles can be observed visually in the LVN-loaded MPs, indicating some portion of the drug was adhered to the surface of the MPs.

Characterization of Silk Fibroin Microneedle Patches. *Scanning Electron Microscopy (SEM) Analysis of Microneedle Patches.* SEM images showed homogeneously shaped MNs with tightly packed porous structures with an average diameter at the base of 493 μm. The needles looked sharp with well-defined structures (Figure 5).

Differential Scanning Calorimetry (DSC) Analysis. Drug polymorphism can lead to variations in physicochemical properties as well as in efficacy.[34] The DSC results of free LVN loaded inside the MNs patches showed the disappearance of the LVN melting peak, which was at 240 °C, in the MNs indicating the absence of free drug (Figure 6).[35] The absence of free drug indicates that the drug added to the microneedles are bound to the silk matrix and not in native crystal forms. The presence of free drug usually increases burst release from the formulations and is generally not desirable for sustained release formulations. Furthermore, DSC thermograms were evaluated in terms of polymorph transitions, as amorphous and crystalline polymorphs of the same molecule might have different efficacy and physicochemical properties. The absence of the exothermic peak at 51−61 °C, showing an amorphous state of levonorgestrel, confirmed that there were no amorphous

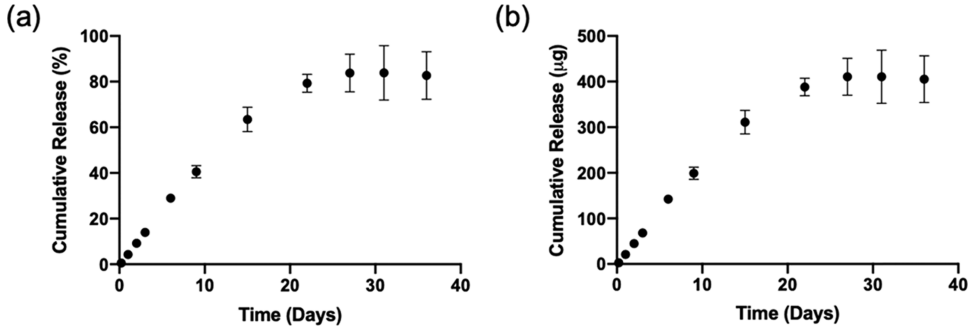

Figure 7. In vitro release profiles of LVN from silk MPs (HMW) under sink conditions in 0.5% SDS solution (45 mL): (a) cumulative release in percentage and (b) cumulative release in micrograms. LVN concentrations in the release media were determined for each time point by HPLC. Data presented are the mean ± SD of a triplicate (n = 3) of release samples.

https://dx.doi.org/10.1021/acsabm.0c00671
ACS Appl. Bio Mater. 2020, 3, 5375−5382

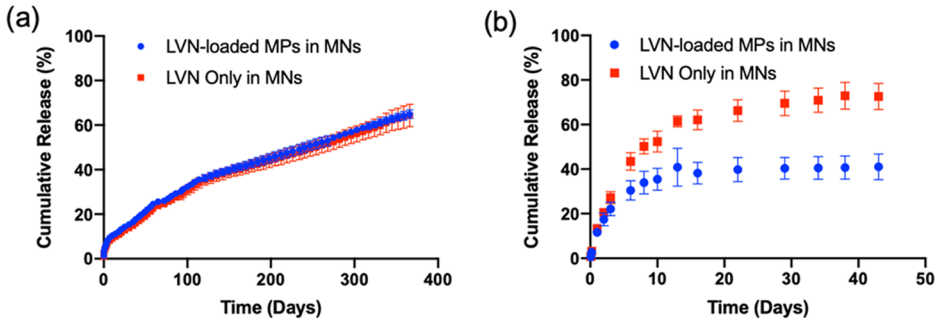

Figure 8. In vitro release profiles of LVN from silk MN patches in: (a) 1 mL PBS, (b) 200 mL of 0.5% SDS solution. LVN concentrations in the release media were determined for each time point by HPLC. Data presented are the mean ± SD of a triplicate (n = 3) of release samples.

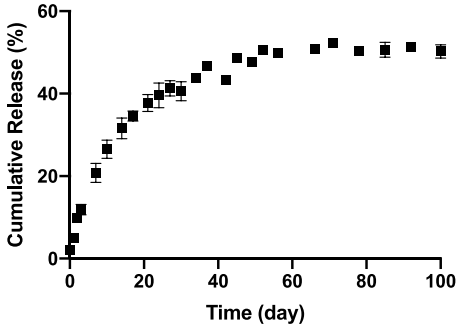

Figure 9. In vitro LVN release from silk—DMSO MNs (3% DMSO, MMW silk) with high-dose LVN in sink conditions (0.5% SDS). Data presented are the mean ± SD of a triplicate (n = 3) of release samples.

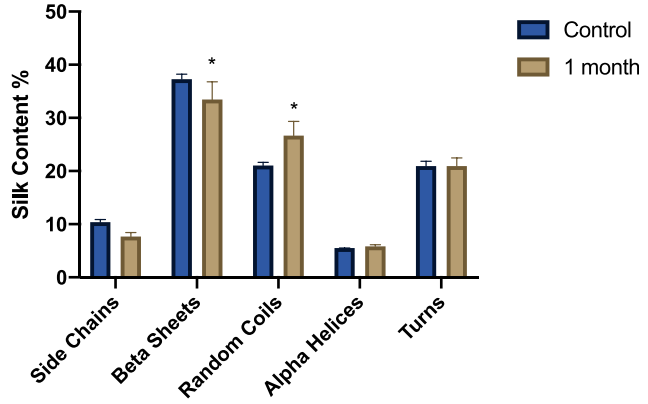

Figure 11. Quantification in percent of the secondary silk structure of the LVN-loaded silk MNs after 0 and 30 days incubation under accelerated aging conditions (40 °C and 75% relative humidity) based on FTIR spectroscopy. (Data presented are mean ± SD of a triplicate (n = 3) of release samples, statistical significance within groups shown with *p < 0.05).

polymorph transitions during the microneedle preparation process.[36]

In Vitro Release Studies. The in vitro release kinetics of LVN from the silk MPs showed that the MPs released LVN continuously for up to one month reaching a total of 405.1 ± 51.3 μg (82.7 ± 10.5%) (Figure 7). The release kinetics of LVN from the MN patches was similar to the MP release (Figure 8). Under nonsink conditions, drug release was controlled by drug solubility and no significant differences were found between the drug-loaded MPs in the MNs and the drug-loaded MNs in terms of release rates. Under sink conditions, the effect of the MPs was observed, where drug release from the MP-loaded MNs was slower than for the drug only MNs. LVN only MNs released 73.3 ± 5.9% of the drug over 43 days, whereas the drug-loaded MPs in the MNs released 41.2 ± 5.8% of the total drug over the same period of time. This data showed that loading MPs did not provide a significant improvement in release profiles or duration, and reduced drug loading. Therefore, formulations were adjusted to increase drug loading to 10 mg by eliminating the MPs and using LVN alone with the addition of 3% DMSO. The in vitro release from the high drug-loading MNs was evaluated under sink conditions (Figure 9). The data showed that LVN was released from the MNs over 93 days and 51.4 ± 1.1% of the drug was released at the end of 3 months. The results indicated that the addition of the DMSO and higher drug loading resulted in slower LVN release as well as higher drug loading.

To provide more control over the release profiles of the drug from the MNs, different silk formulations (concentrations and molecular weights) were studied. The MNs with the highest concentrations of silk (10%, MMW) released the drug at a

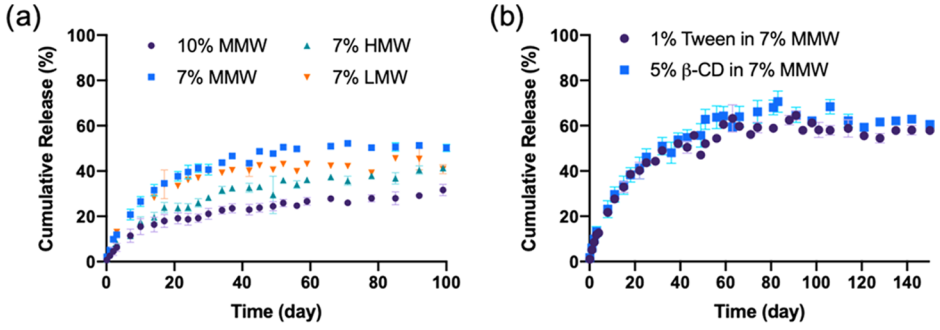

Figure 10. In vitro release profiles of LVN with: (a) different concentrations and molecular weights (MWs) of silk and (b) addition of surfactants. Data presented are the mean ± SD of a triplicate (n = 3) of release samples.

https://dx.doi.org/10.1021/acsabm.0c00671
ACS Appl. Bio Mater. 2020, 3, 5375−5382

slower rate, with a cumulative release of 25.3 ± 1.5% after 100 days. For the MNs at 7% silk concentrations, varying the MW (low, medium, and high) did not have a significant effect on the release profile of the drug after 100 days, with a release of 41.7 ± 3.7, 50.2 ± 1.6, and 41.3 ± 1.1% for low, medium, and high MW, respectively (Figure 10a). After the formulations reached a plateau in terms of release, the MNs were immersed in DMSO to recover residual LVN trapped in the MNs to assess mass balance. Thus, 38.5 ± 12.7% of LVN was recovered for the MNs with the highest silk concentrations, while 40.0 ± 3.7, 76.7 ± 9.6, and 72.5 ± 9.3% was recovered for the low, medium, and high MWs samples, respectively. Finally, the addition of a surfactant and a solubility enhancer such as Tween-20 (1%) and β-cyclodextrin (B-CD, 5%), respectively, added to the silk solution prior to casting for MN formation, provided additional control over the release profiles (Figure 10b). Both formulations led to similar release profiles with a cumulative release of 61.2 ± 1.1 and 62.1 ± 1.7% for the Tween and β-CD, respectively, thus provided an enhanced release compared to the silk formulation without these additives. Indeed, β-cyclodextrin provides a central hydrophobic cavity to host hydrophobic substrates to enhance solubility, while Tween-20 improves drug penetration through the skin as well as modify the hydration of the silk.[37−40]

Stability Study. To ensure the stability of the drug in the MNs, accelerated aging conditions were studied following the guidelines provided by the FDA (Guidance for Industry Q1A(R2) for accelerated stability studies (40 ± 2 °C with 75 ± 5% relative humidity)). MNs prepared with LVN were incubated at 40 °C and 75% relative humidity for 30 days. The patches were then immersed in DMSO, and the recovery of LVN was quantified using HPLC. The recovery at day 0 was 102.6 ± 5.6%, while the recovery after 30 days was 97.6 ± 1.8%; hence, no change in drug stability over time was observed; thus, the MNs would be suitable for long-term storage. Additionally, the main structural features of silk were assessed by FTIR and a slight, but statistically significant, decrease in β-sheet fraction between 1622 and 1637 cm^{-1} was observed, accompanied by an increase in random coil (Figure 11). After 90 days of incubation at 37 °C, no degradation peak could be observed by HPLC, thus the drug remains still active.

CONCLUSIONS

Modifications in the formulation of the silk and the loading of LVN enabled the tuning of the amount of drug loaded and released from silk MN patches over extended periods of time. The release of LVN reached up to 100 days when the drug was loaded directly inside the MNs, while the release extended past a year when the drug was loaded inside MPs prior to casting inside the MN patches. Moreover, all MN formulation delivered LVN above the required daily contraceptive dosage of 30 μg/day.[32] These findings suggest that a long-acting contraception patch based on silk protein materials could be a technology advance enabling broader access to women around the world.

AUTHOR INFORMATION

Corresponding Author

David L. Kaplan − *Department of Biomedical Engineering, Tufts University, Medford, Massachusetts 02155, United States;* orcid.org/0000-0002-9245-7774; Phone: 617-627-3251; Email: david.kaplan@tufts.edu

Authors

Burcin Yavuz − *Department of Biomedical Engineering, Tufts University, Medford, Massachusetts 02155, United States;* orcid.org/0000-0003-2352-9321

Laura Chambre − *Department of Biomedical Engineering, Tufts University, Medford, Massachusetts 02155, United States;* orcid.org/0000-0001-6824-9652

Kristin Harrington − *Department of Biomedical Engineering, Tufts University, Medford, Massachusetts 02155, United States*

Jonathan Kluge − *Vaxess Technologies, Inc., Cambridge, Massachusetts 02139, United States*

Livio Valenti − *Vaxess Technologies, Inc., Cambridge, Massachusetts 02139, United States*

Complete contact information is available at: https://pubs.acs.org/10.1021/acsabm.0c00671

Author Contributions

§B.Y. and L.C. contributed equally to this study. The manuscript was prepared through contributions from all authors.

Notes

The authors declare the following competing financial interest(s): Some of the authors are in a company, Vaxess, and work on related technology, and some own stock in the company.

ACKNOWLEDGMENTS

This study was supported by the Bill and Melinda Gates Foundation (OPP1184023). We would like to thank Anne Valat, Ph.D. for her help with the illustration. Some of the authors are employed by Vaxess Inc., and work on this and related technology and some own stock in the company.

REFERENCES

(1) Sedgh, G.; Singh, S.; Hussain, R. Intended and Unintended Pregnancies Worldwide in 2012 and Recent Trends. *Stud. Fam. Plann.* **2014**, *45*, 301−314.

(2) Bearak, J.; Popinchalk, A.; Alkema, L.; Sedgh, G. Global, Regional, and Subregional Trends in Unintended Pregnancy and Its Outcomes from 1990 to 2014: Estimates from a Bayesian Hierarchical Model. *Lancet Glob. Heal.* **2018**, *6*, 380−389.

(3) Sedgh, G.; Bearak, J.; Singh, S.; Bankole, A.; Popinchalk, A.; Ganatra, B.; Rossier, C.; Gerdts, C.; Tunçalp, Ö.; Johnson, B. R.; Johnston, H. B.; Alkema, L. Abortion Incidence between 1990 and 2014: Global, Regional, and Subregional Levels and Trends. *Lancet* **2016**, *388*, 258−267.

(4) Larrañeta, E.; Lutton, R. E. M.; Woolfson, A. D.; Donnelly, R. F. Microneedle Arrays as Transdermal and Intradermal Drug Delivery Systems: Materials Science, Manufacture and Commercial Development. *Mater. Sci. Eng. R: Rep.* **2016**, *104*, 1−32.

(5) Barry, B. W. Breaching the Skin's Barrier to Drugs. *Nat. Biotechnol.* **2004**, *22*, 165−167.

(6) Eisenstein, M. Something New under the Skin. *Nat. Biotechnol.* **2011**, *29*, 107−109.

(7) Arora, A.; Prausnitz, M. R.; Mitragotri, S. Micro-Scale Devices for Transdermal Drug Delivery. *Int. J. Pharm.* **2008**, *364*, 227−236.

(8) Schoellhammer, C. M.; Blankschtein, D.; Langer, R. Skin Permeabilization for Transdermal Drug Delivery: Recent Advances and Future Prospects. *Expert Opin. Drug Delivery* **2014**, *11*, 393−407.

(9) Han, T.; Das, D. B. Potential of Combined Ultrasound and Microneedles for Enhanced Transdermal Drug Permeation: A Review. *Eur. J. Pharm. Biopharm.* **2015**, *89*, 312−328.

(10) Li, W.; Terry, R. N.; Tang, J.; Feng, M. R.; Schwendeman, S. P.; Prausnitz, M. R. Rapidly Separable Microneedle Patch for the Sustained Release of a Contraceptive. *Nat. Biomed. Eng.* **2019**, *3*, 220−229.

(11) Kamaly, N.; Yameen, B.; Wu, J.; Farokhzad, O. C. Degradable Controlled-Release Polymers and Polymeric Nanoparticles: Mechanisms of Controlling Drug Release. *Chem. Rev.* **2016**, *116*, 2602−2663.
(12) Mohammadi-Samani, S.; Taghipour, B. PLGA Micro and Nanoparticles in Delivery of Peptides and Proteins; Problems and Approaches. *Pharm. Dev. Technol.* **2015**, *20*, 385−393.
(13) Yavuz, B.; Chambre, L.; Kaplan, D. L. Extended Release Formulations Using Silk Proteins for Controlled Delivery of Therapeutics. *Expert Opin. Drug Delivery* **2019**, *16*, 1−16.
(14) Tang, X.; Ding, F.; Yang, Y.; Hu, N.; Wu, H.; Gu, X. Evaluation on in Vitro Biocompatibility of Silk Fibroin-Based Biomaterials with Primarily Cultured Hippocampal Neurons. *J. Biomed. Mater. Res., Part A* **2009**, *91*, 166−174.
(15) Meinel, L.; Hofmann, S.; Karageorgiou, V.; Kirker-Head, C.; McCool, J.; Gronowicz, G.; Zichner, L.; Langer, R.; Vunjak-Novakovic, G.; Kaplan, D. L. The Inflammatory Responses to Silk Films in Vitro and in Vivo. *Biomaterials* **2005**, *26*, 147−155.
(16) Seo, Y.-K.; Yoon, H.-H.; Song, K.-Y.; Kwon, S.-Y.; Lee, H.-S.; Park, Y.-S.; Park, J.-K. Increase in Cell Migration and Angiogenesis in a Composite Silk Scaffold for Tissue-Engineered Ligaments. *J. Orthop. Res.* **2009**, *27*, 495−503.
(17) Yavuz, B.; Zeki, J.; Coburn, J. M.; Ikegaki, N.; Levitin, D.; Kaplan, D. L.; Chiu, B. In Vitro and in Vivo Evaluation of Etoposide - Silk Wafers for Neuroblastoma Treatment. *J. Controlled Release* **2018**, *285*, 162−171.
(18) Yavuz, B.; Morgan, J. L.; Herrera, C.; Harrington, K.; Perez-Ramirez, B.; LiWang, P. J.; Kaplan, D. L. Sustained Release Silk Fibroin Discs: Antibody and Protein Delivery for HIV Prevention. *J. Controlled Release* **2019**, *301*, 1−12.
(19) Yavuz, B.; Zeki, J.; Taylor, J.; Harrington, K.; Coburn, J. M.; Ikegaki, N.; Kaplan, D. L.; Chiu, B. Silk Reservoirs for Local Delivery of Cisplatin for Neuroblastoma Treatment: In Vitro and In Vivo Evaluations. *J. Pharm. Sci.* **2019**, *108*, 2748−2755.
(20) Pritchard, E. M.; Valentin, T.; Panilaitis, B.; Omenetto, F.; Kaplan, D. L. Antibiotic-Releasing Silk Biomaterials for Infection Prevention and Treatment. *Adv. Funct. Mater.* **2013**, *23*, 854−861.
(21) Pritchard, E. M.; Szybala, C.; Boison, D.; Kaplan, D. L. Silk Fibroin Encapsulated Powder Reservoirs for Sustained Release of Adenosine. *J. Controlled Release* **2010**, *144*, 159−167.
(22) Chambre, L.; Parker, R. N.; Allardyce, B. J.; Valente, F.; Rajkhowa, R.; Dilley, R. J.; Wang, X.; Kaplan, D. L. Tunable Biodegradable Silk-Based Memory Foams with Controlled Release of Antibiotics. *ACS Appl. Bio Mater.* **2020**, *3*, 2466−2472.
(23) Tsioris, K.; Raja, W. K.; Pritchard, E. M.; Panilaitis, B.; Kaplan, D. L.; Omenetto, F. G. Fabrication of Silk Microneedles for Controlled-Release Drug Delivery. *Adv. Funct. Mater.* **2012**, *22*, 330−335.
(24) Stinson, J. A.; Raja, W. K.; Lee, S.; Kim, H. B.; Diwan, I.; Tutunjian, S.; Panilaitis, B.; Omenetto, F. G.; Tzipori, S.; Kaplan, D. L. Silk Fibroin Microneedles for Transdermal Vaccine Delivery. *ACS Biomater. Sci. Eng.* **2017**, *3*, 360−369.
(25) Boopathy, A. V.; Mandal, A.; Kulp, D. W.; Menis, S.; Bennett, N. R.; Watkins, H. C.; Wang, W.; Martin, J. T.; Thai, N. T.; He, Y.; Schief, W. R.; Hammond, P. T.; Irvine, D. J. Enhancing Humoral Immunity via Sustained-Release Implantable Microneedle Patch Vaccination. *Proc. Natl. Acad. Sci. U. S. A.* **2019**, *116* (33), 16473−16478.
(26) DeMuth, P. C.; Min, Y.; Irvine, D. J.; Hammond, P. T. Implantable Silk Composite Microneedles for Programmable Vaccine Release Kinetics and Enhanced Immunogenicity in Transcutaneous Immunization. *Adv. Healthcare Mater.* **2014**, *3* (1), 47−58.
(27) Rockwood, D. N.; Preda, R. C.; Yücel, T.; Wang, X.; Lovett, M. L.; Kaplan, D. L. Materials Fabrication from Bombyx Mori Silk Fibroin. *Nat. Protoc.* **2011**, *6*, 1612−1631.
(28) Wray, L. S.; Hu, X.; Gallego, J.; Georgakoudi, I.; Omenetto, F. G.; Schmidt, D.; Kaplan, D. L. Effect of Processing on Silk-Based Biomaterials: Reproducibility and Biocompatibility. *J. Biomed. Mater. Res., Part B* **2011**, *99B* (1), 89.
(29) Wang, X.; Yucel, T.; Lu, Q.; Hu, X.; Kaplan, D. L. Silk Nanospheres and Microspheres from Silk/PVA Blend Films for Drug Delivery. *Biomaterials* **2010**, *31*, 1025−1035.
(30) Hu, X.; Kaplan, D. L.; Cebe, P. Determining Beta-Sheet Crystallinity in Fibrous Proteins by Thermal Analysis and Infrared Spectroscopy. *Macromolecules* **2006**, *39*, 6161−6170.
(31) Gordon, D. J. Mie Scattering by Optically Active Particles. *Biochemistry* **1972**, *11*, 413−420.
(32) Bao, Q.; Gu, B.; Price, C. F.; Zou, Y.; Wang, Y.; Kozak, D.; Choi, S.; Burgess, D. J. Manufacturing and Characterization of Long-Acting Levonorgestrel Intrauterine Systems. *Int. J. Pharm.* **2018**, *550*, 447−454.
(33) Lawrence, B. D.; Wharram, S.; Kluge, J. A.; Leisk, G. G.; Omenetto, F. G.; Rosenblatt, M. I.; Kaplan, D. L. Effect of Hydration on Silk Film Material Properties. *Macromol. Biosci.* **2010**, *10*, 393−403.
(34) Raza, K. Polymorphism: The Phenomenon Affecting the Performance of Drugs. *SOJ Pharm. Pharm. Sci.* **2014**, *1*, No. 10.
(35) Iwashita, S.; Hayashi, H.; Nakagawa, T.; Miyazaki, K. Amorphous Levonorgestrel, Solid Dispersion, and Manufacturing Method for Same. WO Patent WO20141753022014. pp 1−24.
(36) Manoukian, O. S.; Arul, M. R.; Sardashti, N.; Stedman, T.; James, R.; Rudraiah, S.; Kumbar, S. G. Biodegradable Polymeric Injectable Implants for Long-Term Delivery of Contraceptive Drugs. *J. Appl. Polym. Sci.* **2018**, *135*, 46068.
(37) Williams, A. C.; Barry, B. W. Penetration Enhancers. *Adv. Drug Delivery Rev.* **2004**, *56*, 603−618.
(38) Guziewicz, N. A.; Massetti, A. J.; Perez-Ramirez, B. J.; Kaplan, D. L. Mechanisms of Monoclonal Antibody Stabilization and Release from Silk Biomaterials. *Biomaterials* **2013**, *34*, 7766−7775.
(39) Dahan, A.; Miller, J. M.; Hoffman, A.; Amidon, G. E.; Amidon, G. L. The Solubility−Permeability Interplay in Using Cyclodextrins as Pharmaceutical Solubilizers: Mechanistic Modeling and Application to Progesterone. *J. Pharm. Sci.* **2010**, *99*, 2739−2749.
(40) Sivin, I. Risks and Benefits, Advantages and Disadvantages of Levonorgestrel-Releasing Contraceptive Implants. *Drug Saf.* **2003**, *26*, 303−335.

https://dx.doi.org/10.1021/acsabm.0c00671
ACS Appl. Bio Mater. 2020, 3, 5375−5382